

# Analysis of Tooth Surface Elements by Ion Beam Analysis

Victoria Glauche<sup>1)</sup>, Jörg Röhrich<sup>2)</sup>, Wolfgang Böhne<sup>2)</sup>, Ralf J. Radlanski<sup>3)</sup>, Michael Atar<sup>4)</sup>  
Yuma Honda<sup>5)</sup>, Waka Yoshida<sup>5)</sup>, Hatsuhiko Maeda<sup>5)</sup> and Christian H. Finke<sup>1)</sup>

<sup>1)</sup> Department of Pediatric Dentistry, Charité-Universitätsmedizin Berlin, Campus Virchow Klinikum, Germany

<sup>2)</sup> Ion Beam Laboratory ISL, Hahn-Meitner-Institute, Berlin, Germany

<sup>3)</sup> Department of Experimental Dentistry, Charité-Universitätsmedizin Berlin, Campus Benjamin Franklin, Germany

<sup>4)</sup> Department of Oral Growth and Development, Section of Paediatric Dentistry, Barts and The London, Queen Mary University of London, School of Medicine and Dentistry, London, United Kingdom

<sup>5)</sup> Department of Oral Pathology, School of dentistry, Aichi Gakuin University, Center for Advanced Oral Science, Aichi Gakuin University, Japan

**Abstract:** To examine the applicability of elastic recoil detection analysis (ERDA) in studying element constituents of dental hard tissues.

The concentration of all elements using high-energy heavy ions was detected in extracted teeth of both dentitions. The main elements present in enamel (calcium, phosphorus, oxygen, hydrogen), along with nitrogen, carbon, fluorine, sodium, magnesium and zinc, were measured. Concentrations and depth profiles were calculated and compared with simulation data generated using two programs, KONZERN and SIMNRA.

Enamel calcium, phosphorus, oxygen, hydrogen, nitrogen, carbon, fluorine, sodium, magnesium and, occasionally, zinc were detected. One-third of samples showed a constant concentration of the constituents over the analyzed depth, whereas the remaining samples had pronounced surface contaminations of carbon and nitrogen. Although calculation of concentrations with KONZERN gave expected values, simulation with SIMNRA was not possible since no agreement could be obtained between simulated and measured results for the elements.

**Key words:** Dental enamel, Elastic recoil detection analysis, ERDA, Ion beam analysis

## Introduction

The anatomic crown of every tooth is covered by enamel, the most highly mineralized tissue found in the human body. Enamel consists of about 96% inorganic materials, mainly hydroxyapatite crystallites, 4% organic material, and water.<sup>1,2</sup>

The acquired enamel pellicle is an organic film covering the surfaces of teeth which is formed by selective binding of glycoproteins from saliva.<sup>3-5</sup> Proteins, enzymes, immunoglobulins, glucose, and mucins have all been shown to be components of the pellicle. It forms a layer about 0.7-1.0  $\mu\text{m}$  thick and protects enamel by reducing demineralization upon acid challenge. However, it has also been shown to be the means by which microorganisms attach to the tooth leading to the formation of dental plaque and caries.<sup>3,5-7</sup> The earliest sign of a carious lesion is the appearance of a chalky white spot on the surface of the tooth, indicating an area of demineralization of enamel.<sup>8</sup> As the lesion continues to demineralize, it can turn brown and will

eventually turn into a cavitation.<sup>9-13</sup> In the early lesions the surface of the enamel (5-10  $\mu\text{m}$ ) may appear to be intact, despite demineralization processes occurring beneath the surface. Although, these processes are reversible at this stage by means of fluoride application or by increasing uptake of calcium and phosphorus, it is important to gain an insight into the effects of demineralization on tissue elements.<sup>14-18</sup>

The model of an intact surface pellicle covering an area of demineralization has been confirmed by a number of microscopic and radiographic techniques.<sup>19-22</sup> However, none of them assessed whether any changes were occurring within the pellicle itself and the area beneath an intact pellicle. Although a number of nuclear analytical methodologies, such as proton induced x-ray emission (PIXE), particle induced gamma-ray emission, (PIGE), nuclear reaction analysis (NRA), hydrogen NRA (H-NRA), nuclear activation analysis (NAA), or Rutherford backscattering spectroscopy (RBS) are available to investigate these changes, elastic recoil detection analysis (ERDA) is the only technology capable of providing depth profile analyses of all chemical elements found in the outer surface of dental tooth substances

Correspondence to: Prof. Michael Atar, DDS, PhD, MClInDent Sweet Smile Ltd. 21 Shirehall Lane London NW4 2PE United Kingdom Tel.: +44 208 202 1480 Mobile: +44 79 0623 0712, Email: atards@yahoo.com

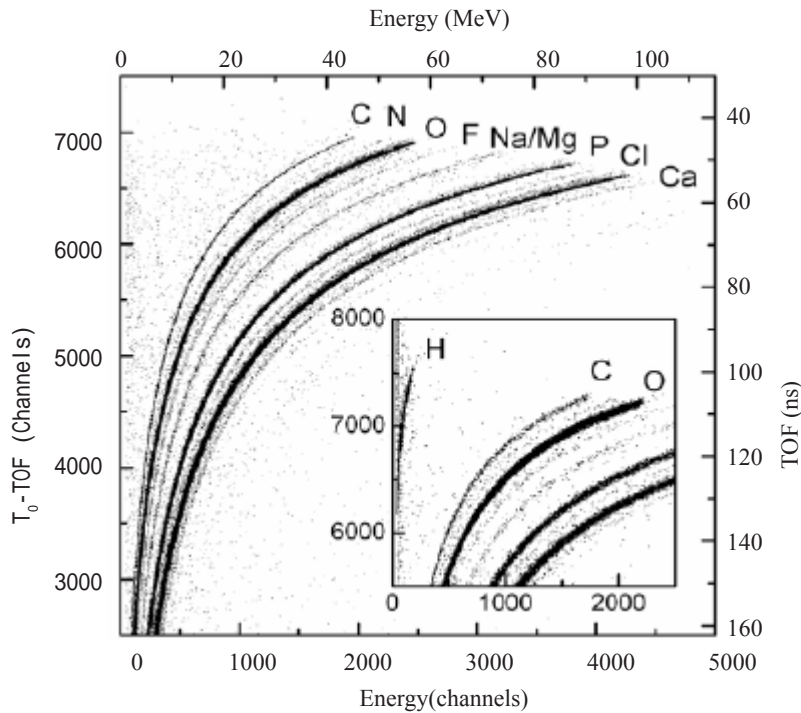


Figure 1. Typical scatterplot of all detected recoils from a measurement of an intact natural tooth surface (21, permanent anterior tooth) with the long TOF spectrometer. The different elements are clearly separated. Insert shows the scatterplot from the measurement of the same spot with the short TOF spectrometer for the determination of hydrogen content.

with good sensitivity.<sup>23-31</sup> This study aims to use ERDA to analyze whether surfaces can be intact after out-diffusion of ions from the subsurface lesion and whether there are consequences of these processes detectable in the early carious lesion.

### Materials and Methods

Seventeen teeth from fourteen dental patients, extracted for orthodontic and other reasons, were used in this study and stored in formalin before use. After rinsing in water, the tooth samples were sawed from buccal to oral, vacuum dried and mounted in a target holder proximal surface uppermost ensuring minimal curvature of the sample.

Elastic recoil detection analysis (ERDA) measurements (Ion-Beam Laboratory ISL of the Hahn-Meitner Institute, Berlin) were performed on healthy and white spot lesions of untreated enamel. ERDA allows the analysis of layer structures used in solid state physics and is based on the Rutherford scattering theory of atomic nuclei.<sup>31</sup> For the measurements, the samples were irradiated with high energy heavy ions in a vacuum of  $10^{-7}$  mbar between 10 minutes and 1 hour. 230 MeV Xe ion beams with ion currents of approximately 2nA and beam spot sizes of  $0.4 \text{ mm}^2$  were used. The measurements were performed at a scattering angle of  $60^\circ$  with a short TOF spectrometer and at an angle of  $40^\circ$  with a long TOF spectrometer.<sup>32</sup> As a result of elastic scattering of the ions,

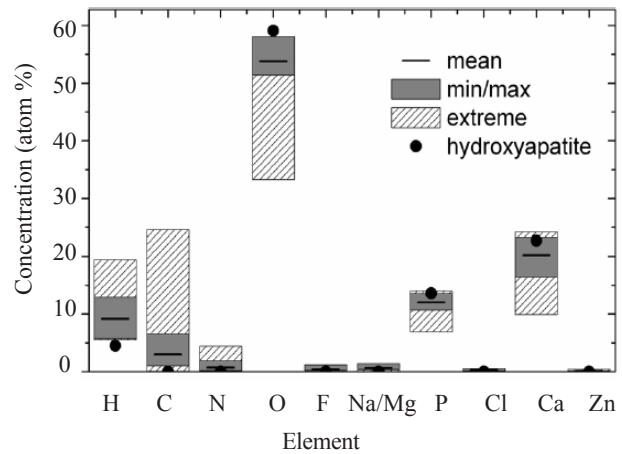


Figure 2. Values for the element concentration for all investigated teeth in atom % calculated with KONZERD.

recoiled sample atoms leave the sample and hit the detector system where the energy and Time-of-Flight (*TOF*) for a fixed distance *s* were measured.

$$\text{Using the formula } E = \frac{M}{2} \left( \frac{s}{TOF} \right)^2$$

where *E* = energy and *M* = mass of the recoiled atoms, an

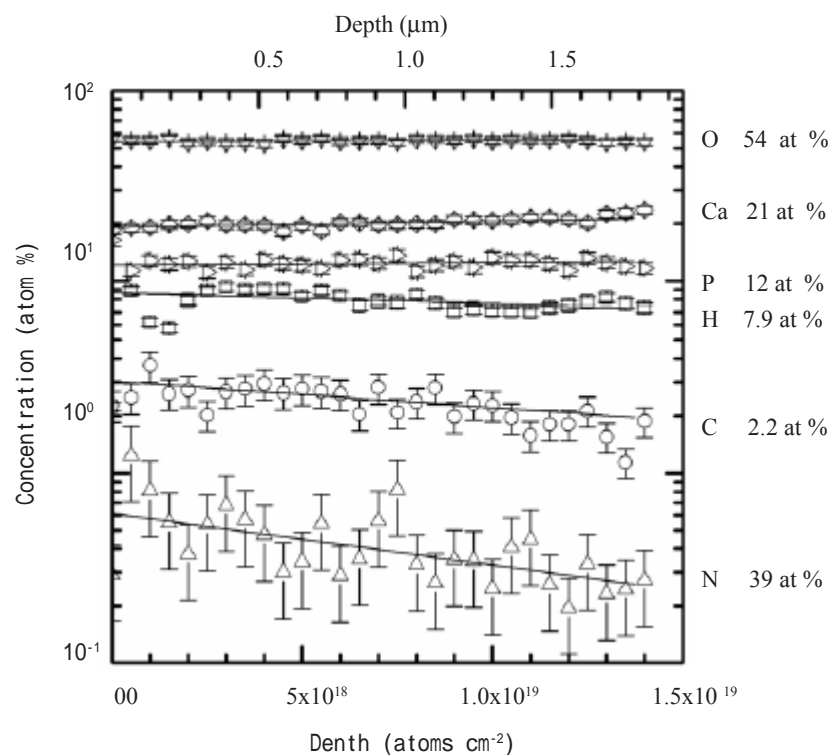


Figure 3. Depth profiles of the main elements for a (18, upper wisdom tooth) tooth calculated with KONZERD. The concentrations of the heavier elements were constant over the analyzed depth. The concentrations of hydrogen, carbon, and nitrogen decrease with increasing depth. The conversion of the calculated area density given in atoms per  $\text{cm}^2$  into a geometrical thickness was performed using a density of  $2.92 \text{ g/cm}^3$  for hydroxyapatite and the averaged concentrations are shown.

identification and separation of the various atomic elements in a 2-dimensional plot of time vs. energy could be recorded. This, in turn, allowed the energy spectra for each element of the sample to be obtained. Sample composition, element concentration and depth profiles were calculated from the energy spectra directly and by means of simulation using the computer programs KONZERD<sup>33</sup> and SIMNRA.<sup>34</sup>

To investigate the effect of tooth surface roughness on the measurements taken from the untreated enamel samples, further studies were performed to allow comparisons with that of polished tooth samples. Three additional teeth were embedded in resin (brand of resin-Buehler GmbH, Düsseldorf), sawed with a low-revving saw and polished with diamond-studded paper with decreasing grain size and, finally, silicon carbide foil with a grain size of  $0.3 \mu\text{m}$ . Quality was confirmed using light and scanning electron microscopy (SEM, CamScan MaXim2040S, CamScan Electron Optics Ltd, USA).

### Results

Enamel calcium, phosphorus, oxygen, hydrogen, nitrogen, carbon, fluorine, sodium, magnesium, and occasionally, zinc were detected. *Figure 1* depicts a typical graph of the detected atoms of a healthy tooth surface. The recoils with the maximum energy of a particular mass originate from the surface. The energy reduces

with increasing depth. The density of the points reflects the corresponding element concentration in the tooth.

A third of the samples showed a constant concentration of the constituents over the analyzed depth, whereas the remaining samples had pronounced surface contaminations of carbon and nitrogen. The minimum and maximum element concentrations were calculated with the program KONZERD and averaged over a depth range from  $2 \cdot 10^{18} \text{ atoms cm}^{-2}$  to  $12 \cdot 10^{18} \text{ atoms cm}^{-2}$ , allowing possible contributions from surface contaminations to be avoided (*Figure 2*). Extreme values from samples with very high carbon contamination were excluded from averaging but are included for comparison.

From *Figure 2*, it can be seen that the teeth consisted of about 90 atom % (at %) hydroxyapatite. The residual 10 at % was composed mainly of hydrogen, carbon and other elements with fractions of less than 1 at % each. A higher than expected hydrogen excess of about 5 at % compared to pure hydroxyapatite was detected. The mean values for the concentration of the main components, except hydrogen, were in reasonable agreement with the theoretical values assuming pure hydroxyapatite ( $\text{Ca}_{10}(\text{PO}_4)_6(\text{OH})_2$ ) (*Figure 3*). Despite the best possible selection of samples the slopes of the simulated spectra did not match the measured ones. However, this affected all elements simultaneously, allowing determination of the concentrations with

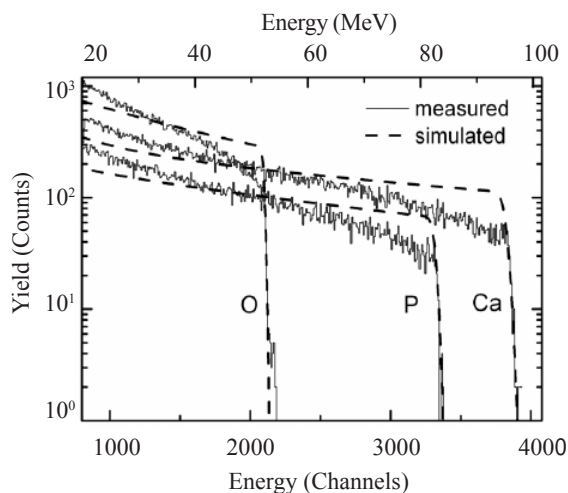


Figure 4. Measured (open symbols) and simulated (line) energy spectra of the main elements for a measurement of a (55, second upper primary molar) tooth. The high energetic edges correspond to the surface and lower energy to increased depth. The calcium atoms with 20 MeV arise from a depth of about 1.5  $\mu\text{m}$ . The different slopes of the measured and simulated spectra are evident.

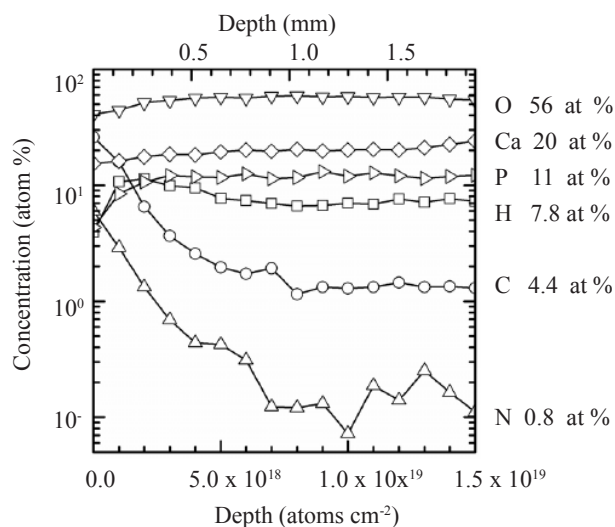


Figure 5. Depth profiles of the main elements for a (55, second upper primary molar) tooth calculated with KONZARD. The concentrations of carbon and nitrogen decrease steeply from the surface to the bulk, indicating the existence of a film on top of the tooth surface. The averaged concentrations are given for comparison.

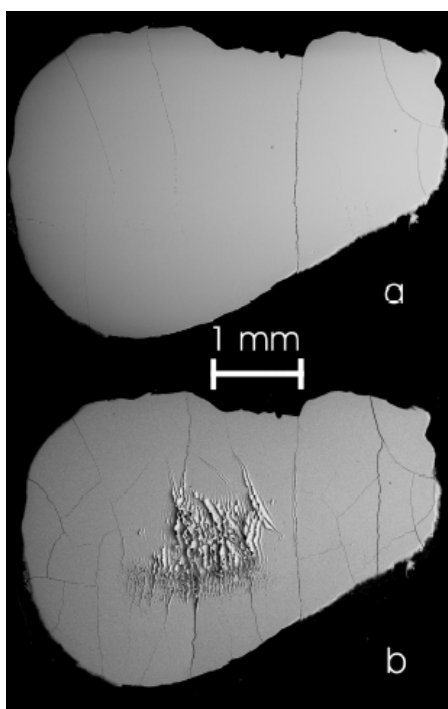


Figure 6. Scanning electron micrograph (SEM) pictures of a polished tooth 65 cut (a) before and (b) after two ERDA measurements with 230 MeV Xe ions. The total fluence amounts to about  $3.6 \cdot 10^{14}$  ions/cm<sup>2</sup>. Besides the increased number of micro cracks, the formation of waves perpendicular to the beam direction is visible. The overlapping of the two beam spots is reflected in the different heights of the wave structures.

KONZARD. Although the calculation of the concentrations with KONZARD gave expected values (Figure 3), simulation with SIMNRA was not possible since no agreement could be obtained between simulated and measured results for the elements (Figure 4). Simulation of oxygen, phosphorus, and calcium spectra in a second deciduous molar (55: deciduous tooth) measured with the long TOF spectrometer and assuming a constant concentration for all elements, gave a steeper slope than for the measured values. The assumption of a depth dependent concentration for the elements did not solve the problem, since the effect occurred for all element spectra.

Concentration depth profiles of the main elements for a tooth (55, second upper primary molar) were calculated with KONZARD (Figure 5). It can be seen that the concentrations of carbon and nitrogen decreased steeply from the surface to the bulk, indicating the existence of a structure that is not part of the tooth structure probably the dental biofilm (pellicle). In addition, a correlation between the carbon and nitrogen concentrations was evident.

Light microscopy and SEM were used to investigate the effect of tooth surface roughness on the measurements (Figure 6). With both methods some cracks were found, which were shown to increase if the specimens were submitted to high vacuum. Furthermore, small scratches from the cutting were detected. SEM pictures taken before and after the measurement showed superficial roughness and wave forming on the beam spot area.

## Discussion

The main enamel components have been reported as calcium

(38%), phosphorus (18%), magnesium (0.4%), carbon dioxide (2.5%), water (3%), and organic substances (1%).<sup>35–38</sup> Many studies using methodologies such as atomic force microscopy (AFM), PIXE or quantitative light-induced fluorescence (QLF) were unable to measure oxygen levels, despite it being a major component in enamel, since the analytical methodology involve carbonization of the samples.<sup>39–43</sup> In contrast, ERDA does not involve any manipulation of the samples and, therefore, has the capability to measure the total atomic concentration of all constituents within the sample. In addition, ERDA allows the quantification of both hydrogen and oxygen within the sample.

The excess hydrogen observed in the samples was interesting since there was no evidence of additional chemically bonded water in the samples as the oxygen values were not in excess. It is possible that the hydrogen excess was derived from organic material within the sample. This is supported by the value obtained for carbon content of approximately 3 at %, which gave a ratio of 2:1 hydrogen: carbon as observed in organic matter. It is also possible that the nitrogen originated from organic material, particularly since a correlation between the carbon and nitrogen content was observed in the samples. Previous studies have reported the fraction of carbon dioxide as 2.5 weight % which corresponds to 1.4 at % carbon.<sup>2, 20, 44</sup> This value agrees with the minimum value obtained in this study and would suggest that some of the carbon in the samples represented superficial contamination. The fluorine concentration in the samples was consistent with other studies, though factors such as the fluoride content of drinking water, dentition, and methodology used may affect the actual values obtained in individual studies.<sup>20, 45, 46</sup> Concentrations of trace elements such as chlorine, sodium, magnesium and zinc were generally consistent with other studies.<sup>47, 48</sup>

Although the applicability of ERDA for the chemical characterization of tooth surfaces could be demonstrated, a comparative analysis of sound and demineralized enamel was hindered by a number of factors which could be attributable to the properties of the samples. Since ERDA is a highly sensitive technique, any surface contamination of the sample may result in varying element concentrations. Some of the variations seen between samples in this study reflect contamination by the dental biofilm or formalin attached at the dental biofilm. Similarly, changes in sample composition such as cracking, release of water and gaseous reaction products during the irradiation, ion beam analysis or vacuum in the scattering chamber may account for some of the sampling variation. Another important factor was the influence of surface geometry on the measurements. A plane and smooth sampling surface was assumed for the calculations which is not the case for natural tooth surfaces. Although rigorous attempts were made to ensure optimal samples, the slopes of the simulated spectra did not match the measured ones suggesting

that surface roughness of the teeth was affecting the measured values. However, this affected all elements simultaneously and allowed the determination of the concentrations with KONZERD, though concentrations could not be determined by SIMNRA. Attempts to investigate the effect of surface roughness using SEM showed the formation of waves in the analysis area. This has been demonstrated using ion irradiation where amorphous solids showed the formation of waves following bombardment with phosphates being particularly sensitive to ion irradiation.<sup>49, 50</sup> The induced roughness was dependent on the number of particles, which in this study led to a measurement time dependent difference between simulated and measured spectra. Since the ion beam affected the samples, the only way to improve the analysis was to reduce the number of impinging primary ions for the measurement which, in turn, led to an increase in the concentration errors and inaccuracies in the concentration depth profiles. The individual effects of each of these factors were difficult to predict and made assumptions for the simulation analysis practically impossible.

### Conclusions

EDRA allowed detection of all elements in expected concentrations, with the exception of natural teeth covered by the dental biofilm, where high carbon and nitrogen values were obtained. Due to factors that significantly influence the measurements, ERDA is unsuitable as a standard investigative tool for analyzing the main elements of dental enamel.

### Acknowledgements

Research was partly supported by a grant from the research support fund of the Humboldt University (99724150/98-184 Ionenstrahlanalytik am ISL).

The authors would like to thank Dr. Klaumünzer from the HMI for helpful discussions on materials modification with ion beams.

### References

1. Fincham AG, Moradian-Oldak J and Simmer JP. The structural biology of the developing dental enamel matrix. *J Struct Biol* 126: 270–299, 1999
2. Schroeder HE. Structure and biology of the gingivo-dental area. *J Am Dent Hyg Assoc* 45: 378–379, 1971
3. Hannig M and Joiner A. The structure, function and properties of the acquired pellicle. *Monogr Oral Sci* 19: 29–64, 2006
4. Hannig C, Hannig M and Attin T. Enzymes in the acquired enamel pellicle. *Eur J Oral Sci* 113: 2–13, 2005
5. Lendenmann U, Grogan J and Oppenheim FG. Saliva and dental pellicle – A review. *Adv Dent Res* 14: 22–28, 2000
6. Hicks J, Garcia-Godoy F and Flaitz C. Biological factors in dental caries: role of saliva and dental plaque in the dynamic process of demineralization and remineralization. *J Clin*

- Pediatr Dent 28: 47–52, 2003
7. Featherstone JD. The continuum of dental caries – evidence for a dynamic disease process. *J Dent Res* 83: C39–42, 2004.
  8. Arends J and Christoffersen J. The nature of early caries lesions in enamel. *J Dent Res* 65: 2–11, 1986
  9. Angmar-Mansson B and ten Bosch JJ. Advances in methods for diagnosing coronal caries - a review. *Adv Dent Res* 7: 70–79, 1993
  10. Arnold WH, Gaengler P, Sabov K, Schmitz I, Gedalia I and Steinberg D. Induction and 3D reconstruction of caries-like lesions in an experimental dental plaque biofilm model. *J Oral Rehabil* 28: 748–754, 2000
  11. Bader JD and Brown JP. Dilemmas in caries diagnosis. *J Am Dent Assoc* 124: 48–50, 1993
  12. Featherstone JD. Caries detection and prevention with laser energy. *Dent Clin North Am* 44: 955–969, 2000
  13. Margolis HC, Zhang YP, Lee CY, Kent RL Jr and Moreno EC. Kinetics of enamel demineralization in vitro. *J Dent Res* 78: 1326–1335, 1999
  14. Hellwig C and Lennon AM. Systemic versus topical fluoride. *Caries Res* 38: 258–262, 2004
  15. Attin T, Kielbassa AM, Schwanenberg M and Hellwig E. Effect of fluoride treatment on remineralization of bleached enamel. *J Oral Rehabil* 24: 282–286, 1997
  16. Dean HT. Fluorine in the control of dental caries. *J Am Dent Assoc*, 52: 1–8, 1956.
  17. Seow WK. Clinical diagnosis of enamel defects: pitfalls and practical guidelines. *Int Dent J* 47: 173–182, 1997.
  18. Stookey GK, Jackson RD, Zandona AG and Analoui M. Dental caries diagnosis. *Dent Clin of North Am* 43: 665–677, 1999
  19. Pitts NB and Rimmer P A. An in vivo comparison of radiographic and directly assessed clinical caries status of posterior approximal surfaces in primer and permanent teeth. *Caries Res* 26: 146–152, 1992
  20. Driessens FC, Theuns HM, Heijligers HJ and Borggreven JM. Microradiography and electron microprobe analysis of some natural white and brown spot enamel lesions with and without laminations. *Caries Res* 20: 398–405, 1986
  21. Eggertsson H, Analoui M, van der Veen MH, González-Cabezas C, Eckert G and Stookey G. Detection of early interproximal caries in vitro using laser fluorescence, dye-enhanced laser fluorescence and direct visual examination. *Caries Res* 33: 227–223, 1999
  22. Hicks MJ and Silverstone LM. Acid-etching of caries-like lesions of enamel: a polarized light microscopic study *Caries Res* 18: 315–326, 1984
  23. Moller B and Carlsson LE. Particle-induced X-ray emission (PIXE) analysis of trace elements in human coronal dentin. *Swed Dent J* 8: 67–72, 1984
  24. Maenhaut W. Multielement analysis of biological materials by particle-induced x-ray emission (PIXE). *Scanning Microsc* 4: 43–59, 1990
  25. Campbell JL. Use of charged particle beams for analysis of biological tissues and fluids. *Neurotoxicology* 4: 1–12, 1983
  26. Moretto P. Nuclear microprobe: a microanalytical technique in biology. *Cell Mol Biol (Noisy-le-grand)* 42: 1–16, 1996.
  27. Weise HP, Gorner W and Hedrich M. Determination of elements by nuclear analytical methods. *Fresenius J Anal Chem* 369: 8–14, 2001
  28. Chaudhri MA. Nuclear analytical methods in calcified tissue research. *Nutrition*, 11: 538–541 1995
  29. Versieck J. Neutron activation analysis for the determination of trace elements in biological materials. *Biol Trace Elem Res* 43-45: 407–413, 1994
  30. Dollinger G, Bergmaier A, Faestermann T and Frey CM. High resolution depth profile analysis by elastic recoil detection with heavy ions. *Anal Bioanal Chem* 353: 311–315, 1995
  31. Tesmer JR and Natasi M. Handbook of Modern Ion Beam Materials. Materials Research Society, 1995 Pittsburgh
  32. Bohne W, Röhrich J and Röschert G. The Berlin time-of-flight ERDA setup. *Nucl Instrum Methods Phys Res B* 136-138: 633–637, 1985
  33. Bergmaier A, Dollinger G and Frey CM. Quantitative elastic recoil detection. *Nucl Instrum Methods Phys Res B* 99: 488, 1995
  34. Mayer M. SIMNRA Users Guide. Garching: Max-Planck Institut für Plasmaphysik 1997, publication no. IPP 9/113.
  35. Weatherall JA. Composition of dental enamel. *Br Med Bull* 31: 115–119, 1975
  36. Angmar B, Carlstrom D and Glas JE. Studies on the ultrastructure of dental enamel IV. The mineralization of normal human enamel. *J Ultrastruct Res* 8: 12–23, 1963.
  37. ten Cate JM, Dundon KA, Vernon PG, Damato FA, Huntington E, Exterkate RA, Wefel JS, Jordan T, Stephen KW and Roberts AJ. Preparation and measurement of artificial enamel lesions, a four-laboratory ring test. *Caries Res* 30: 400–407, 1996
  38. Ngo H, Ruben J, Arends J, White D, Mount GJ, Peters MC, Faller RV and Pfarrer A. Electron probe microanalysis and transverse microradiography studies of artificial lesions in enamel and dentin: a comparative study. *Adv Dent Res* 11: 426–432, 1997
  39. Farina M, Schemmel A, Weissmuller G, Cruz R, Kachar B and Bisch PM. Atomic force microscopy study of tooth surfaces. *J Struct Biol* 125: 39–49, 1999
  40. Jones KW, Annegarn HJ and Sellschop JP. Charged particle analysis of fluorine distributions in human tooth enamel. *Arch Oral Biol* 23: 31–37, 1978

41. Arshed W, Akanle OA and Spyrou NM. The distribution of fluorine and other elements in teeth using proton induced reaction analysis techniques. *J Radioanal Nucl Chem* 179: 349–355, 1994
42. Lane DW and Peach DF. Some observations on the trace element concentrations in human dental enamel. *Biol Trace Elem Res* 60: 1–11, 1997
43. Tranaeus S, Al-Khateeb S, Bjorkman S, Twetman S and Angmar-Månsson B. Application of quantitative light-induced fluorescence to monitor incipient lesions in caries-active children. A comparative study of remineralisation by fluoride varnish and professional cleaning. *Eur J Oral Sci* 109: 71–75, 2001
44. Driessens FC, Theuns HM, Heijligers HJ and Borggreven JM. Microradiography and electron-microprobe analysis of some caries-like lesions of enamel prepared in vitro in human teeth. *Arch Oral Biol* 31: 837–840, 1986
45. Petersson LG, Odellius H, Lodding A, Larsson SJ and Frostell G. Ion probe study of fluorine gradients in outermost layers of human enamel. *J Dent Res* 55: 980–990, 1976
46. Nakagaki H, Koyama Y, Sakakibara Y, Weatherell JA and Robinson C. Distribution of fluoride across human dental enamel, dentine and cementum. *Arch Oral Biol* 32: 651–654, 1987
47. Reitznerová E, Amarasiriwardena D, Kopcáková M and Barnes RM. Determination of some trace elements in human tooth enamel. *Fresenius J Anal Chem* 367: 748–754, 2000
48. Gierat-Kucharzewska B, Braziewicz J, Majewska U, Gózdź S and Karasinski A. Concentration of selected elements in the roots and crowns of both primary and permanent teeth with caries disease. *Biol Trace Elem Res* 96: 159–167, 2003
49. Klaumünzer S and Benyagoub A. Phenomenology of the plastic flow of amorphous solids induced by heavy-ion bombardment. *Phys Rev B Condens Matter* 43: 7502–7506, 1991
50. Gutzmann A, Klaumünzer S and Meier P. Ion-beam-induced surface instability of glassy Fe<sub>40</sub>Ni<sub>40</sub>B<sub>20</sub>. *Phys Rev Lett* 74: 2256–2259, 1995